Nano Energy 78 (2020) 105291

Contents lists available at ScienceDirect

Nano Energy

journal homepage: http://www.elsevier.com/locate/nanoen

Advanced triboelectric nanogenerator with multi-mode energy harvesting and anti-impact properties for smart glove and wearable e-textile

Sheng Wang [a,b], Shuai Liu [a], Jianyu Zhou [a], Faxin Li [c], Jun Li [b], Xufeng Cao [a], Zhiyuan Li [b], Junshuo Zhang [a], Binshang Li [b], Yu Wang [a], Xinglong Gong [a,*]

[a] CAS Key Laboratory of Mechanical Behavior and Design of Materials, Department of Modern Mechanics, CAS Center for Excellence in Complex System Mechanics, University of Science and Technology of China (USTC), Hefei, 230027, PR China
[b] Anhui Weiwei Rubber Parts Group Co. Ltd., Tongcheng, 231400, Anhui, China
[c] LTCS and College of Engineering, Peking University, Beijing, 100871, China

ARTICLE INFO

Keywords:
Triboelectric nanogenerator
Multi-mode
External-field sensing
Safeguard
Smart electronics

ABSTRACT

Environmental hazardous stimuli including strong electromagnetic field and impact force were always harmful to human beings. Developing functional triboelectric nanogenerator (TENG) with universally harvesting various energy and anti-impact effect may be an effective strategy to collect energy as well as protect human beings from danger. Thus, a miniaturized all-in-one TENG with high structural durability, anti-impact and multi-mode harvesting energy from compression, swaying and magnetic field was developed by assembling shear thickening fluid (STF) and magneto-sensitive films. TENG yielded maximum power density of 27.05 mW/m^2 with the voltage of 10.40 V at 10 MΩ under compression. It also sensed and collected tiny STF flowing energy under non-contact mode. Besides, high magnetic-sensitive effect endowed TENG with magnetic dependent programmable shapes which enabled it to harvest non-contact rubbing/deformation energy. More importantly, the device with STF exhibited high anti-impact properties which could resist and dissipate harsh collision force from 1390 N to 409 N, demonstrating excellent safeguarding properties for TENG and human wearers. This versatile device also showed reliable sensing properties to various external magnetic field, human motions, contacted materials and impact forces. In addition, a wearable TENG-based smart glove as a self-powered functional sensor presented the ability of precisely mapping finger joints. Finally, newly-designed Kevlar/TENG-based e-textile arrays with 95% impact-force dissipating and multi-fields display performance was proposed. Thus, this work opened a new perspective for the development of functional TENGs as wearable electronic devices in universally energy-scavenging and safeguarding areas.

1. Introduction

The continuous flourish in personal smart device aggravates the energy crisis in recent years which urgently motivates the development of new energy sources. Fulfilling the satisfaction of energy demand is more and more significant in wearable electronics [1–4]. Considered as a promising alternative to substitute or partially replace traditional power system, triboelectric nanogenerator (TENG), based on the coupling mechanism of triboelectrification and electrostatic induction, is a device which can effectively harvest and transform ambient mechanical energy into electricity [5–8]. As the outstanding superiority of affordability, environmental friendliness and needless of frequent replacement, it shows profound applications in renewable energy source to power various electronics, wearable self-powered sensors, robotics, health-care monitoring [9–17]. However, traditional wearable TENGs are usually independently valid in designed modes which fail to gather other forms of abundantly available energy. So functional TENGs with universal and high efficiency in collecting and sensing multiple energy under various stimuli is still highly preferable [18–21].

Integrating and miniaturized portable TENGs with the requirement of maximizing gaining multi-directional energy manifests the TENGs have to long-term expose and sustain various mechanical excitations such as compression, twisting, wind blowing and water dropping [22–26]. These adverse triggers easily destroy and fail TENG devices. Currently, novel developed liquid-solid non-contact TENGs with high endurance showed longer lifespan [27–29]. As wearable devices, they

* Corresponding author.
E-mail address: gongxl@ustc.edu.cn (X. Gong).

https://doi.org/10.1016/j.nanoen.2020.105291
Received 17 June 2020; Received in revised form 1 August 2020; Accepted 11 August 2020
Available online 20 August 2020

could collect compression/rubbing mechanical energy and detect various human movements under non-contact mode [30,31]. However, multi-field stimuli and energy sill accompany in daily life which some are seriously dangerous to humans. For example, harsh collision and impact from sports to car accidents happened in our daily life may result in serious physical hurt. Besides, electromagnetic field, as one of the most familiar hazards sources, is widespread around outdoor, mineral area and working machines. Invisible strong electromagnetic field is especially harmful to pregnant, patients and old people. On the other hand, external impact is also harmful to the most reported flexible TENGs. Mechanical fatigue and structure damage led by kinetic strike also seriously shorten lifespan of TENG device. Fortunately, the increasing awareness of personal safety consciousness now urgently propel to develop functional multi-mode TENG to harvest as well as monitor external hazard energy. For example, several hybrid nanogenerators with triboelectric-electromagnetic effect could act as sensors to detect external magnetic field, but the complicated and stiff structures impeded their application as wearable electronics [32–36]. Recently, newly developed shapeable ferro-fluid-based TENG owned the sensing capabilities to strong magnetic field [37]. A bionic stretchable nanogenerator could harvest water flow energy and act as a self-powered sensor to detect danger underwater which could be used to rescue people [38]. Regrettably, such a smart functional TENG system with multi-mode energy-harvesting, high safeguarding properties and the based self-powered sensor to analyze various danger stimuli has not been developed so far.

Shear thickening fluid (STF) is a smart material which composes of nanoparticles dispersing phase and liquid solvent. It is a liquid in natural state. However, the particles gather together to form frictional contact network at high loading rate and the viscosity dramatically increases, leading to a solid state [39,40]. Owing to the reversible and rate-dependent mechanical property, STF has been applied in various areas including damper, vibration controlling and safeguards [41–43]. So one effective strategy to overcome the structural fragility and provide protection to human beings is to combine high friction materials with TENGs. Inspired by the liquid-solid transition effect, introducing STF with high force-dissipation ability into TENG may endow the device with multi-manner energy-collecting, enhanced structural durability and better anti-impact effect.

In this work, a multi-mode energy-harvesting and safeguarding TENG based on STF and magneto-sensitive film was constructed. The TENG exhibited high-energy harvesting effect which the maximum power density was 27.05 mW/m^2 under compression. Owing to the fluidity of STF and magnetic field-responsive character of ecoflex/CI, TENG also enabled to sense and gather energy from liquid flow and magnetic-responsive film deformations. Besides, single TENG with high energy-dissipation effect also restrained and reduced impact force by 70.58%. As a functional self-powered sensor, it shows conspicuous detecting effect to various excitations. In addition, TENG-based smart glove and textile electronics with self-powered monitoring external-field and safeguarding properties were systematically investigated. In conclusion, the advanced TENG as well as the based wearable devices shows significant potentials in new power sources, smart robots, healthcare and safeguards.

2. Experimental sections

2.1. Materials and preparation of TENGs

Firstly, carbonyl irons (CIs) were added into the ecoflex-0020 (Smooth-On Inc) with stirring and the mixture were then poured into the 3D-printed mould followed by curing at 55 °C for 20 min. Finally, the Ecoflex/CI films with thickness of 0.8 mm were peeled off and worked as magnetic sensitive shell.

The conductive PDMS/MWCNT/CI layer was prepared by dispersing 3% of multi-walled carbon (MWCNT) into PDMS matrix with magnetically stirring for 3 h. Then CI particles and the curing agent were added followed by mixing for 0.5 h. The mixture with conductive wires were molded into metal mould and cured at 90 °C for 10 min.

The preparation procedure of polystyrene-ethylacrylate (PST-EA)-based STF was as followed. Styrene (purified by NaOH solution), ethyl acrylate, acrylate and distill water were mixed in a 500 ml three-necked flask with reflexing and N_2 conditions for 0.5 h. Then small amount of the recrystallized potassium persulfate (KPS) were added into the solution and stirred for another 10 min. The flask was then moved into a water bath (75 °C) and reacted for 6 h. After cooling to room temperature, the emulsion was centrifuged, sonicated and washed by water for 3 times. The solid PST-EA nano-particles were obtained after vacuum drying treatment. Uniform STF solution was fabricated by dispersing PST-EA nano-particles into ethylene glycol and milled by a ball crusher for 24 h. In this work, the fraction of STF particles were 54%, 56% and 58%, respectively.

The TENG device was fabricated by assembling ecoflex/CI shell and STF with PDMS/MWCNT/CI by using ecoflex/CI pro-cure matrix. Then they were cured at 50 °C for 10 min.

2.2. Characterization systems

Nano/mirco-structures of the composites were characterized by SEM (Gemini SEM 500, ZEISS). The shear thickening effect of STF and magnetorheological properties of ecoflex/CI were all tested by using a commercial rheometer (Physica MCR 301, Anton Paar Co., Austria). The triboelectric performance of the device were recorded by a digital multimeter and the voltage signals were all processed by low-pass filtering method to filter out equipment high-frequency noise signal. Besides, 3 digital multimeters were used to successively measure all the mapping units of the smart glove and wearable e-textile arrays in this work. A drop hammer test system was applied to conduct the impact tests.

3. Results and discussion

3.1. Multi-mode energy harvesting and sensing properties of TENG device

The preparation procedures of TENG were presented in Fig. 1a–c. Briefly, ecoflex and CI were uniformly mixed and dropped into the molud (Fig. 1a). After curing at 50 °C for 20 min, the film shell was peeled off and assembled with PST-EA-based STF and PDMS/MWCNT/CI (Fig. 1b). Air bubbles were partially squeezed to form structural depression on Ecoflex/CI (Fig. 1c, e). This structure was beneficial for the deformation of polymer shell under the excitation of magnetic force. Air and STF were all encapsulated in TENG (Fig. 1d). SEM image of pristine MWCNT was shown in Fig. 1f. Shapes of the synthesis PST-EA nano-particles were uniform which the diameter was about 400 nm (Fig. 1g). Magnetic CI fillers were about 3 μm (Fig. 1h). Surface of ecoflex/CI-10% was smooth (Fig. 1i) and more CI particles appeared on ecoflex/CI-50% (Fig. 1j). Large numbers of MWCNT were on PDMS/MWCNT/CI (Fig. 1k). The well dispersed MWCNT formed effective conductive path which was favorable for conductivity.

In this work, different fractions of STF have been prepared for optimizing the STF performance. The rheological properties in Fig. 1l clearly showed the viscosity firstly decreased with the increase of shear rates, presenting shear thinning property. After reaching a critical shear value, viscosity were increased dramatically which behaved shear thickening (ST) effect. Especially, the initial viscosity of STF with the volume fraction of 56% was as low as 14.73 Pa.s. However, its maximum viscosity was as high as 175.61 Pa.s which STF could not flow and present rigid state. The initial viscosity of STF-58% was higher which had adverse effect on the fluidity of STF. The maximum viscosity of STF-54% was lower. Thus, STF-56% was appropriate for TENG device.

In addition, magnetic field dependent rheological performance of Ecoflex/CI films were also studied. The composites showed fast response

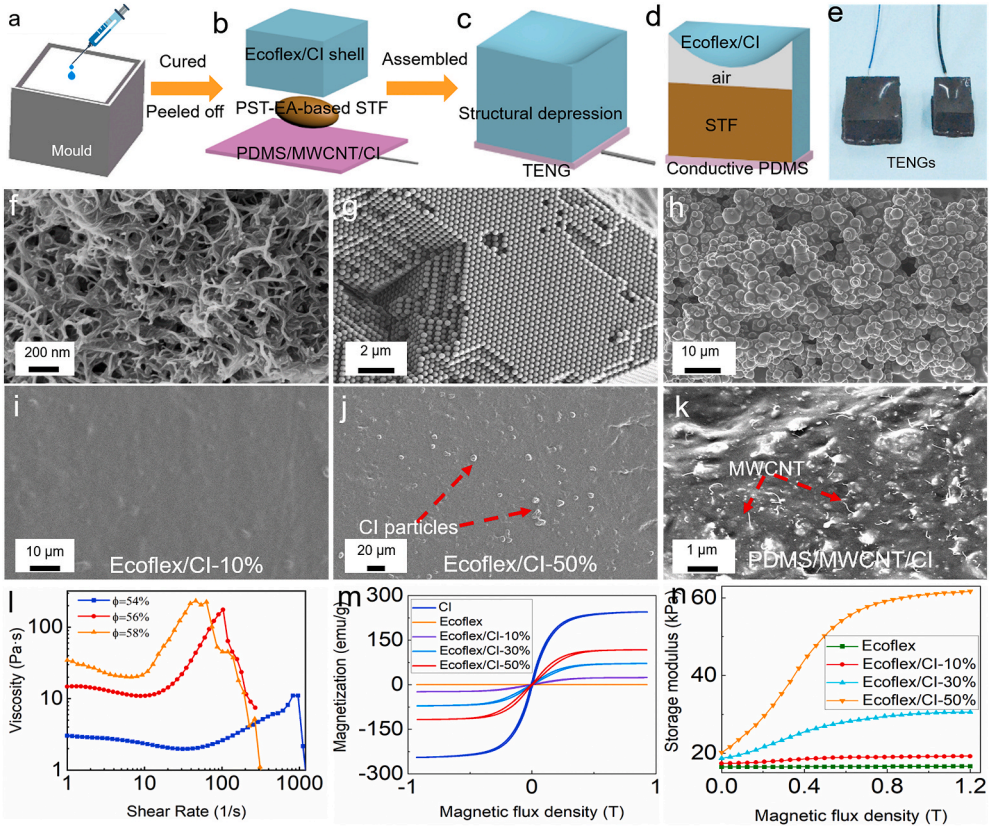

Fig. 1. (a) Preparation procedures of the TENG device: un-cured ecoflex/CI were dropped on the mould, (b, c, e) STF, ecoflex/CI and PDMS/MWCNT/CI were assembled and cured into TENG, (d) schematic of the components of TENG. SEM images of (f) MWCNT, (g) PST-EA nano-particles, (h) CI micro-fillers, (i) ecoflex/CI-10%, (j) ecoflex/CI-50% and (k) PDMS/MWCNT/CI conductive layer. (l) Shear thickening effect of STF, magnetic responsive rheological properties of the as-prepared composites: (m) the magnetic hysteresis loops (n) and MR effect.

to magnetic field which their storage modulus (G') increased with the increasing of magnetic field (Fig. 1n). CI particles also showed positive influence on the magnetorheological (MR) effect. Especially, the maximum G′ of Ecoflex/CI-50% was as high as 61.67 kPa and the magnetorheological effect was 205.60%. As for pure ecoflex, the rheological properties were independent of magnetic field which the initial and maximum storage modulus were 16.46 and 16.62 kPa, respectively.

This high magnetic responsive property was mainly because of the remarkable intrinsic magnetization of CI particles. All ecoflex/CI composites presented typical soft magnetic effect which the saturated magnetization values of Ecoflex/CI with CI fraction of 10%, 30% and 50% were 23.74, 71.23 and 117.04 emu g^{-1} respectively. As for ecoflex, its magnetization kept at 0.21 emu g^{-1} (Fig. 1m). Thus, Ecoflex/CI-50% showed remarkable magnetic field dependent effect.

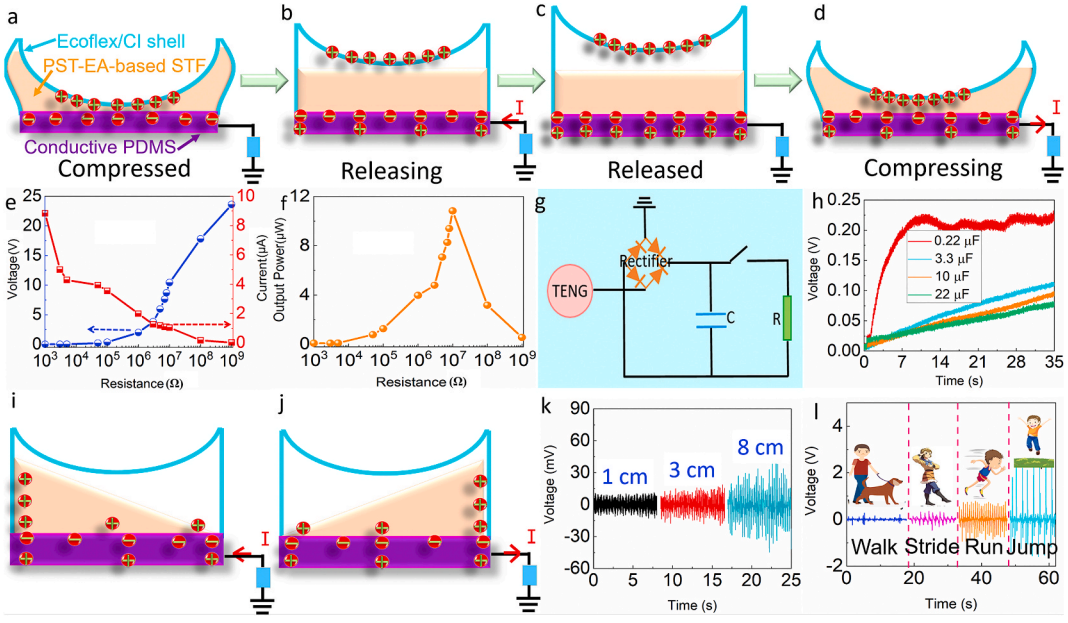

Fig. 2. (a–d) Working mechanism of TENG under compression, resistance dependent (e) triboelectric voltage, current and (f) output power, (g) a circuit diagram composed of TENG, rectifier, charging capacitors, resistance and (h) the corresponding charging curves. (i, j) Electrons transferred during STF flowing process and (k) the corresponding voltages, (l) human sensing properties of wearable TENG under non-contact swaying mode.

The mechanism of TENG relied on the triboelectricfication and electrostatic induction [18,44–47]. The upper ecoflex/CI film contacted with conductive PDMS layer, generating the electron transformation between the surfaces (Fig. 2a). After the positive ecoflex/CI left, redundant electrons on PDMS layer led a potential difference between the polymer and ground. Thus, electrical current occurred by the electron flow (Fig. 2b). After all the free electrons flew away, the system turned to equilibrium and no current could be measured (Fig. 2c). When ecoflex/CI returned to conductive PDMS again, the enhanced potential on the back side of PDMS enabled to drive electrons to flow back from the ground. So an opposite current signal was generated until TENG reverted to pristine state (Fig. 2d). On this occasion, the TENG could harvest and transform mechanical energy into electricity.

The resistance dependent triboelectric performance of TENG (2 × 2 × 1 cm^3) was firstly investigated under oscillator compression mode. The loading frequency and force were 10 Hz and 60 N, respectively. Undoubtedly, the voltages increased sharply when external load resistance was higher than 10^5 Ω and the maximum value was 23.59 V (1 GΩ, Fig. 2e). Several voltage signals were presented in Fig. S1a and the maximum voltage at 10 MΩ were stable under cyclic loading-unloading excitations (Fig. S1b). However, the current showed the opposite tendency which it decreased with the increasing of resistance. The maximum current was 8.84 μA at 1 kΩ. As calculated in Fig. 2f, the output power firstly increased with the increasing of resistance and after reaching a maximum value, it stared to decrease. The maximum power density was 27.05 mW/m^2 with the voltage and resistance of 10.40 V and 10 MΩ. So the as-prepared TENG was capable of harvesting compression mechanical energy and worked as a power source to light up LEDs (Movie 1).

Supplementary video related to this article can be found at https://doi.org/10.1016/j.nanoen.2020.105291

A circuit diagram comprising of TENG, rectifier, capacitors and resistance was presented to study the charging properties (Fig. 2g). Once TENG charged capacitor, the voltage with 0.22 μF capacitor reached to 0.23 V within 30 s (Fig. 2h).

Compared with traditional "solid-solid" TENGs, "liquid-solid" TENGs owned the advantages of slight friction interaction between interfaces and longer lifespan [27,48]. Since STF was in liquid state, it also fluently flew which manifested electrons transferred between inner sidewalls. Firstly, TENG was fixed on an end of cantilever and an oscillator was applied to load the stimuli (Fig. S2a). Enclosed STFs swayed, rubbed the polymers, leading to electron transformation and outputting currents (Fig. 2i and j). When the swaying amplitude was 1 cm, the voltage was 11.3 mV and it finally gained to 46.9 mV as the amplitude varied to 8 cm (Fig. 2k). It also presented ideal stability even excited for 200 s (Fig. S2b). So the proposed liquid-solid TENG proved to harvest and convert slight STF-flow mechanical energy into electricity under non-contacted-mode.

Besides, owing to the different arm swaying amplitudes and speeds generated by human movements, this portable TENG showed potential ability to sense various human gestures and motions (Fig. 2l). The TENG worn on human finger outputted a voltage of 0.28 V during walking process. With the increasing of swing amplitudes, the voltages changed to 0.47 V, 1.01 V and 2.52 V with striding, running and jumping processes. Simultaneously, it also showed fast response to external excitation which the signal frequencies of running is much higher than the other movements. In this regard, the TENG device could effectively sense and collect kinetic energy into electricity, uncompromising the mechanical fatigues or damage, which worked as new power source and portable self-powered sensor.

Embedding stimuli-responsive soft CI particles into polymer matrix endowed external films with magnetic actuation property [49]. A commercial magnet was applied to load the magnetic field (Fig. S3) and the field simulation was exhibited in Fig. 3i. TENG displayed magnetically programmable configuration owing to the high magnetization responsive property (Fig. 3a–h). Ecoflex/CI shell was driven to deform

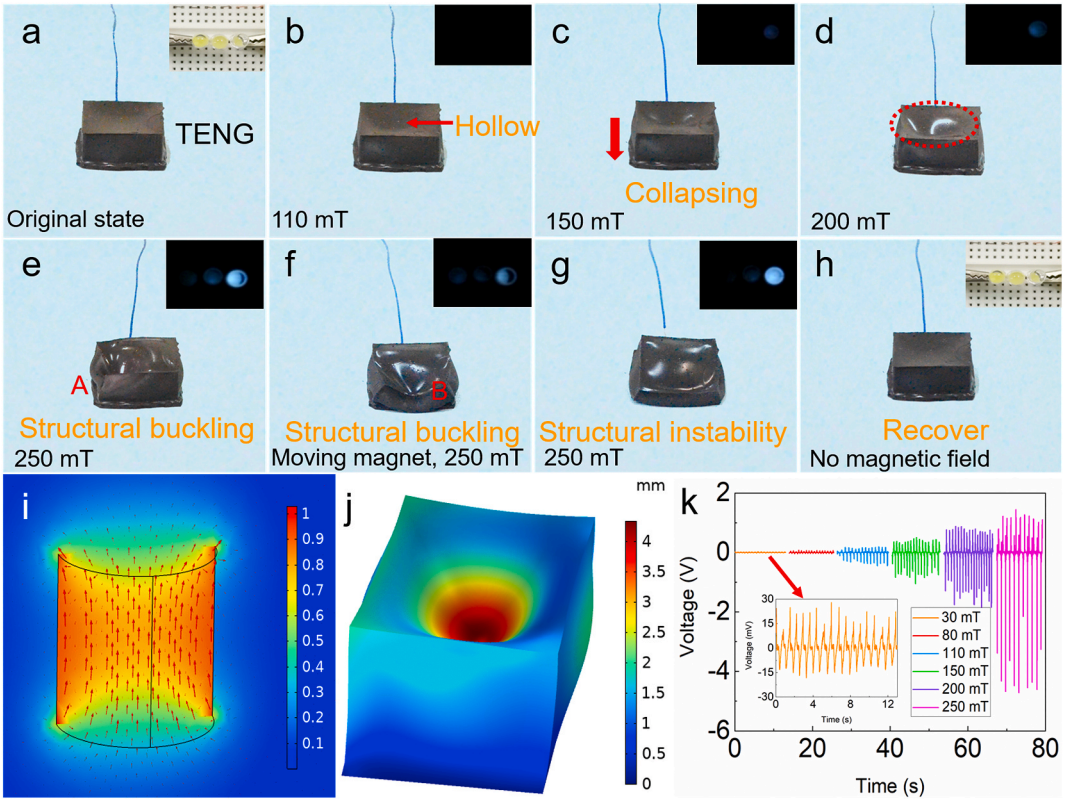

Fig. 3. (a–h) Deformation process of TENG under the excitation of magnetic field, the simulation of (i) magnet and (j) ecoflex/CI shell, (k) magnetic dependent triboelectric performance.

and retain a certain shape by magnetic forces (Fig. 3d–g) and the displacement field was also shown in Fig. 3j. However, it immediately relaxed to original state once unloading magnetic field (Fig. 3h). During the deformation, TENG gathered the mechanical energy and outputted voltage signals. LEDs connected with the TENG could be lit up and the light intensity increased with the increasing deformation. The light intensity also could manefist the variation of deformation and outputting voltages in these processes (insert figures in Fig. 3a–h) (Movie S2).

Supplementary video related to this article can be found at https://doi.org/10.1016/j.nanoen.2020.105291

The magnetic field-dependent triboelectric performance under non-contact-mode showed the output voltage was 28.1 mV at 30 mT (Fig. 3k). These cyclic peaks indicated the TENG with high sensitivity and reliability could even sense and harvest slight mechanical deformations triggered by magnetic fields. The voltages were undoubtedly increased with magnetic forces and finally reached 4.71 V at 250 mT. In conclusion, the as-designed TENG device with functional stimuli-responsive triboelectric properties was more desirable as an intelligent power source and bi-mode sensor platform for actuating low-power electronic devices and sensing complex multi-fields in multi-field conditions.

Flexible tactile sensors, mimicking the perception properties of human skin, are smart systems which enable to quantifying sense various contacted materials and environmental changes. Considering the safeguarding and high sensitivity to force, mechanical-electrical properties of the as-prepared TENG was comprehensively explored on quasi-static and dynamic impact conditions. Fig. 4a showed a typical voltage signal-time curve during the contact-release process of TENG. The voltages by touching PU sponge (Fig. 4b), river stone (Fig. 4c) and PDMS (Fig. 4d) were different owing to their distinguished tribo-electrification. The other contacted materials and the corresponding voltage comparison were also presented (Fig. 4e, f, Fig. S4). In this regard, the wearable TENG, as smart e-skin, could feel and detect various external materials through physical contact.

In addition, owing to the introduction of STF, the anti-impact as well as energy-harvesting properties under harsh collision conditions were further explored. A drop hammer impactor system reported in previous work has been applied [50]. Clearly, the maximum force loaded on force sensor was high and a rebound peak appeared after the first impact (Fig. 4g and h). As for ecoflex/CI film, the maximum impact force was decreased and a similar tendency was also presented. This demonstrated the force sensor and ecoflex/CI film could dissipate small amount of energy. As an important protective component, STF could effectively absorb and dissipate external collision force which the maximum force has be undoubtedly reduced to as low as 409 N and there was no second peak which also proved its high efficiency in absorbing energy. So the safeguarding properties under different impact forces were studied. The maximum forces loaded directly on force sensor were 823 N, 1133 N and 1390 N at the falling heights of 10–30 cm (Fig. 4i, Fig. S5). However, they decreased to 128 N, 304 N and 409 N if loaded on TENG, indicating its distinguished safeguarding property. As a self-powered force sensor, the TENG could generate 0.43 V, 1.51 V and 2.96 V during impact processes (Fig. 4j). This result proved the TENG device could work at various conditions as a soft self-powered force sensor and safeguarding protector for portable smart electronics.

3.2. TENG-based wearable glove with self-powered monitoring performance

Human hands are vital tools in daily life. The finger joints are so skillful that many works are accomplished relying on our hands. The frequently used joints everyday also involve large numbers of tiny mechanical energies. However, it is also possible for hands to get injured during work. Thus, it is inspiring preferable to develop novel TENG-based glove with energy-collecting as well as precisely monitoring various external stimuli. Simultaneously, accurately real-time

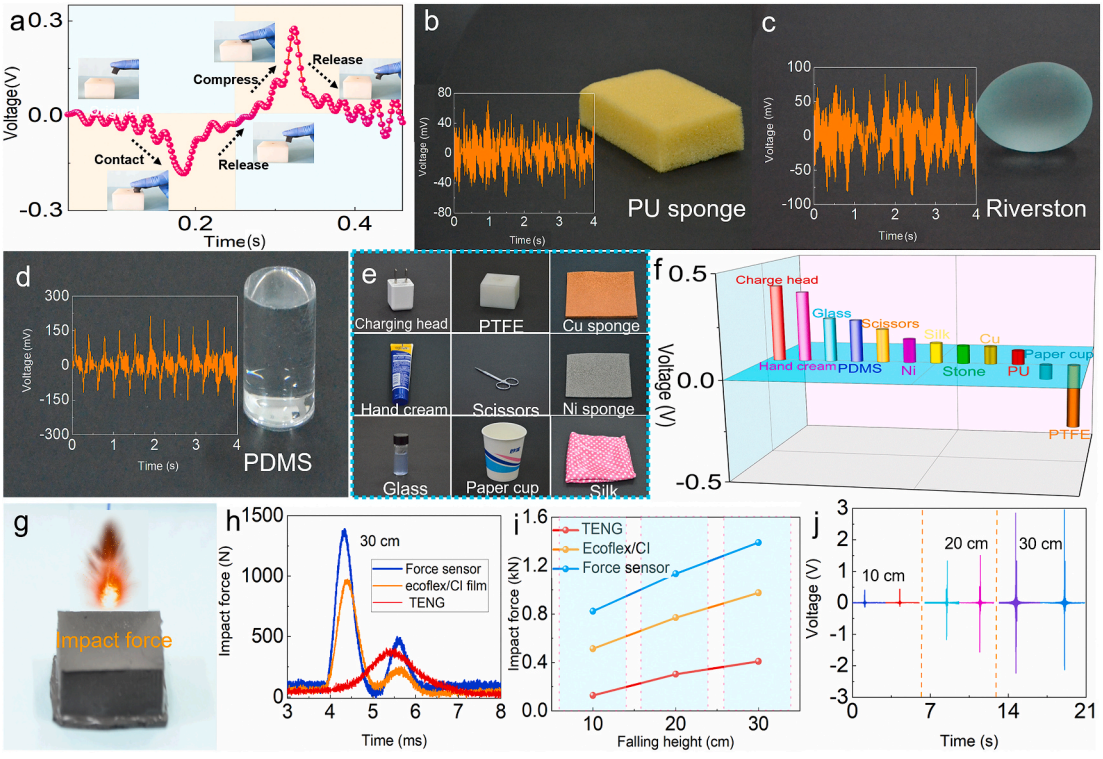

Fig. 4. (a) Voltage signal of TENG as a portable e-skin when gently contacting PTFE. Tactile cognition of (b) PU sponge, (c) river stone, (d) PDMS and (e) other contacted materials, (f) the corresponding voltage comparison. (g) Anti-impact as well as triboelectric performance of TENG under harsh impact excitation: (h) representative force curves comparison of TENG, ecoflex/CI and force sensor impacted from 30 cm height, (i) falling height dependent impact forces and (j) the corresponding triboelectric voltages of TENG during loading process.

monitoring all the complex deformations and gestures of joints is crucial in human health-care training treatments [51]. Here, a TENG-based human hand array has been developed (Fig. 5a). TENGs were assembled on a hand-mould (Fig. S6) and uncured ecoflex/CI was poured and cured to connect the array. It was comfortably worn on hand and the high flexibility guaranteed its adapting to complex mechanical deformations. TENGs sensed the bending excitation (Fig. 5b) and the maximum output voltages were 80.57 mV, 39.54 mV and 17.57 mV (Fig. 5c, Fig. S7). The array on the back of hand with 3 × 3 units also enabled to perceive and display different compression forces (Fig. 5d and e). The maximum voltage generated by the center TENG was 0.76 V, manifesting its sustaining the largest compression force. Thus, the real-time pressure recognition mapping of the hand array under finger bending (Fig. 5f), grasping ring box (Fig. 5g) and apple (Fig. 5h) were presented. Under middle/ring finger bending, the voltages were slight (Fig. 5i). However, once grasping rigid box, the signals increased and the distribution could be used to assess the compression forces of finger joints (Fig. 5j). The maximum voltage was 1.45 V which exhibited the thumb sustained the maximum force during grasping process. Similarly, the voltage mapping in Fig. 5k could also provide the force distribution of grasping apple. In conclusion, the hand array with high sensitivity, self-powered real-time monitoring properties allowed its potential application in smart robots, wearable human health-care and safety alert areas.

3.3. *Anti-impact and voltage response of multifunctional Kevlar/TENG pads to various external excitations*

External impact from collision and strike always occurred in daily life which often led to damages and hurt. To sense the danger and protect human being from injury, various protective materials have been studied [52,53]. Particularly, Kevlar fibers with ultrahigh tensile modulus and ideal bending deformation is a promising candidate for developing novel portable TENG devices with energy-harvesting and safeguarding properties. Thus, wearable Kevlar/TENG pad have been fabricated to further explore the multi-function under impact conditions. Firstly, single Kevlar/TENG (Fig. 6a), without compromising its flexibility (Fig. 6b), could be worn on human body (Fig. 6c). To mimic the anti-impact effect, a stone was applied to compress it from different falling heights and a force sensor was used to record the impact force (Fig. 6d). Interestingly, the dissipated forces by Kevlar/TENG were dramatically lower than those directly loaded on force sensor, indicating the as-designed array showing high efficiency in absorbing impact energy (Fig. 6e). The output voltages of Kevlar/TENG were undoubtedly increased from 0.84 to 2.18 V as the impact height varied from 10 to 30 cm, showing force-sensing effect (Fig. 6f).

Therefore, the mechanic-electric performance of Kevlar/TENG array as smart wearable e-textile were explored (Fig. 6g). 9 TENGs with 5 × 5 cm^2 were decorated on a Kevlar via simple sewing processes and the 4 edges were sewed with zippers (Fig. 6h). Drop hammer test system was applied to load the impact excitation. Keeping the falling height at 40 cm, the impact force loaded directly on the force sensor was as high as 2080 N. Energy dissipation effect of 1 and 4 Kevlar fibers, 1 and 4 Kevlar/ecoflex/CI (ecoflex/CI films were directly fixed on Kevlar) were slight which the forces were decreased to 2000 N, 1920 N, 1880 N and 1400 N, respectively (Fig. 6j). Second rebound peaks could be observed in these curves which also indicated much kinetic energy were residual after the first impact. However, the force was dramatically reduced to 520 N once dissipated by 1 Kevlar/TENG array and no second rebound curve appeared which indicated most of the energy were absorbed. The device also showed high reliable and stable mechanical properties during 7 cyclic loading-unloading impacts (Fig. 6k). Undoubtedly, it decreased to as low as 90 N if impacting on 4 overlying Kevlar/TENGs (Fig. 6i) and the buffer time (duration of the force peak, Fig. S8a, b) was increased to 12.9 ms (force sensor: 1.2 ms, 1 Kevlar/TENG: 3.5 ms, Fig. S8c). 4 stacked Kevlar/TENG pads remarkably absorbed the impact energy owing to the high energy-dissipating effect of STFs. The corresponding output voltage of the uppermost device was 12.23 V and it kept

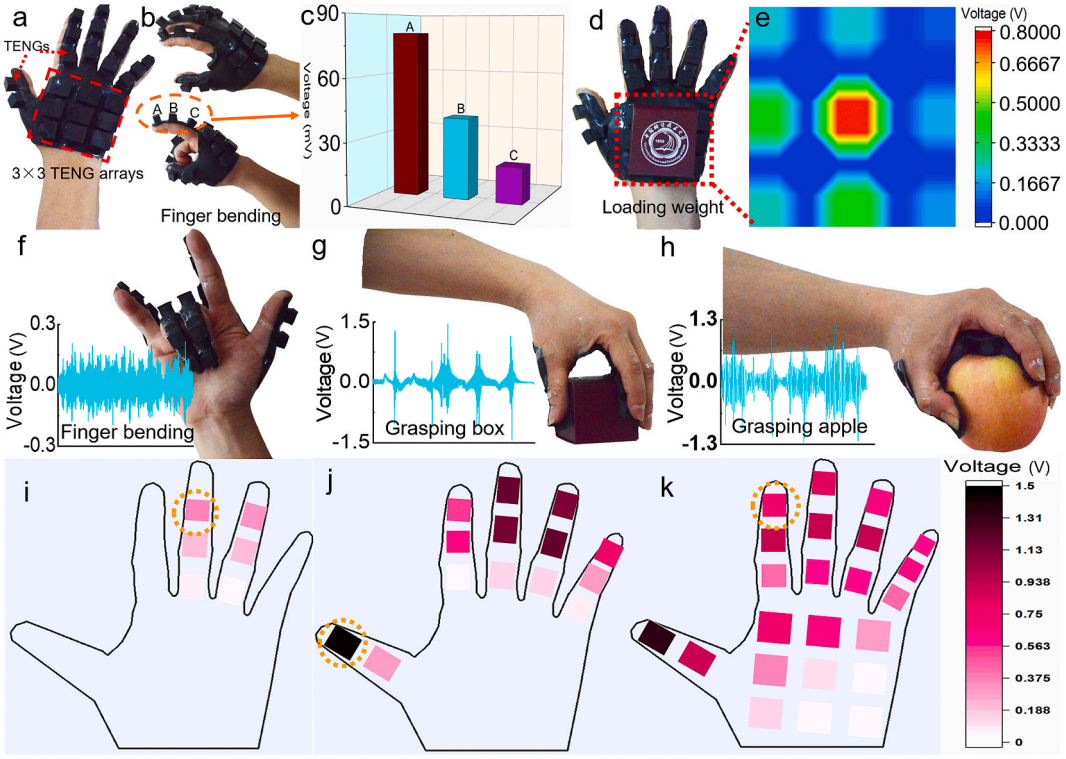

Fig. 5. (a) A TENG-based hand array, human gesture sensing performance of the device: (b) index finger bending and (c) the corresponding maximum voltages, (d, e) pressure distribution of the array on the back of hand. Demonstration of the array as a self-powered sensor for the precisely recognizing various finger movements: (f) finger bending gesture, (g) grasping box, (h) apple and (i–k) the corresponding force sensing mappings.

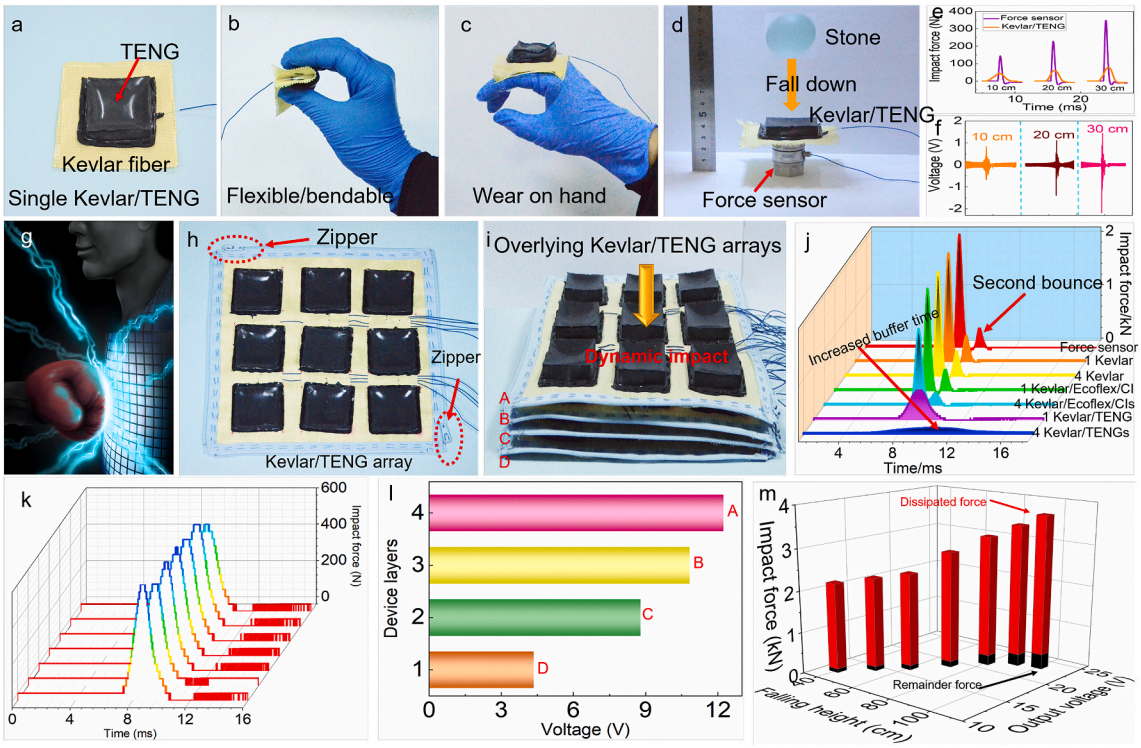

Fig. 6. (a) Single Kevlar/TENG could (b) be bent and (c) worn. (d) Photo, (e) loading forces and (f) output voltages of the anti-impact properties of Kevlar/TENG by a stone falling from 10 to 30 cm. (g) Schematic of the wearable Kevlar/TENG array with safeguarding and triboelectric properties under impact: (h) single and (i) overlying Kevlar/TENG arrays, (j) impact force curves loaded by drop hammer on different materials at the falling height of 40 cm and (k) the mechanical stability of 1 Kevlar/TENG, (l) the output voltages of the 4 layers of overlying array pads; (m) safeguarding as well as the force sensing properties of the overlying array in the 3D bar graph.

decreasing which also indicated the loading force were gradually dissipated by STFs (Fig. 6l). Finally, the falling height dependent triboelectric and protection performance of 4 layered Kevlar/TENG pads in low velocity impact tests were systematically investigated. TENG was mounted on the metal force sensor to record the impact force after collision. From Fig. 6m, the impact force loaded on the force sensor was 2240 N (falling height 60 cm) while it significantly reduced to 110 N (decreased by 95.09%) after the dissipation of the pads. Similarly, the maximum force loaded on the force sensor was 3360 N (impact falling from 100 cm). In comparison, the remainder force on pads was decreased to 360 N, proving excellent anti-impact properties. On the other hand, triboelectric voltages increased with the increasing of impact energy which it was 16.41 V at dropping height of 60 cm and finally reached 23.31 V at 100 cm, presenting outstanding impact force-monitoring properties. Thus, this favorable anti-impact/multi-sensing property allowed Kevlar/TENG as a wearable functional electronics to provide more reliable physical protection under emergent kinetic harm and the self-powered monitoring performance helped to sense and assess various tactile violations.

On behalf of the light weight and high flexibility, the as-designed Kevlar/TENG array was shape-programmable. The bendable array (Fig. 7a-I) could be comfortably worn on human arm (Fig. 7a-II). Two arrays could be assembled together by tightening the zippers (Fig. S9 a-b) and worn on leg (Fig. 7a-III). Four arrays were designed to various configurations which could be wrapped around on the waist (Fig. S9 c, Fig. 7a-IV). The larger pad provided large protection clothing area (Fig. 7a-V) and it could be folded into overlying textile (Fig. S9 d). According to the above result, the stacked arrays in Fig. 7a-VI offered higher safeguarding property for human being in emergencies. In addition, this smart garment electronics also demonstrated versatility in sensing various external excitations. Owing to the flowability of STF, it generated and outputted electrical signals (Fig. 7j) during the arm-swing process (Fig. 7b). The maximum voltages were stable (Fig. 7f), indicating the array could be used to detect human non-contacted movements such as walking and running. On the other hand, TENGs were attracted to deform once a magnet moved (Fig. 7c). This multi-mode Kevlar/TENG also assessed surrounding magnetic field variation by outputting tiny signals. From Fig. 7k, the magnet moving route could be clearly displayed in the voltage mapping, exhibiting its high sensitivity to magnetic field. Besides, under compression (Fig. 7d) and impact (Fig. 7e), the array also enabled to accurately monitor the position and force distribution by the pixel voltages in Fig. 7l and m, respectively. Especially, the maximum voltage signals under arm-swing, magnetic field excitation, compression and hammer impact were 0.25 V, 16.64 mV, 11.02 V and 18.54 V, respectively (Fig. 7f–i). These signals were all very stable which manifested their reliable self-powered sensing effect to various dangerous stimuli. To this end, this wearable shape-adaptable Kevlar/TENG pad with self-powered properties and safeguarding effect was favorable as intelligent clothing in robots, human-machine interaction, health-care and protection areas.

4. Conclusion

This work reported a versatile TENG with impact/sway/magnetic field multi-mode energy harvesting and protective properties. STF showed typical rate-dependent mechanical property which the initial and maximum viscosity were 14.73 and 175.61 Pa.s, respectively. TENG obtained the maximum power density of 27.05 mW/m^2 with resistance of 10 MΩ under compression. Furthermore, the as-prepared TENG was also capable of harvesting liquid-swing kinetic energy and deformation energy triggered by magnetic fields. Besides energy-collecting and self-powered sensing external multi-field properties, this novel TENG has been proven to effectively absorb and dissipate collision energy, providing excellent protective property for wearers. In addition, this

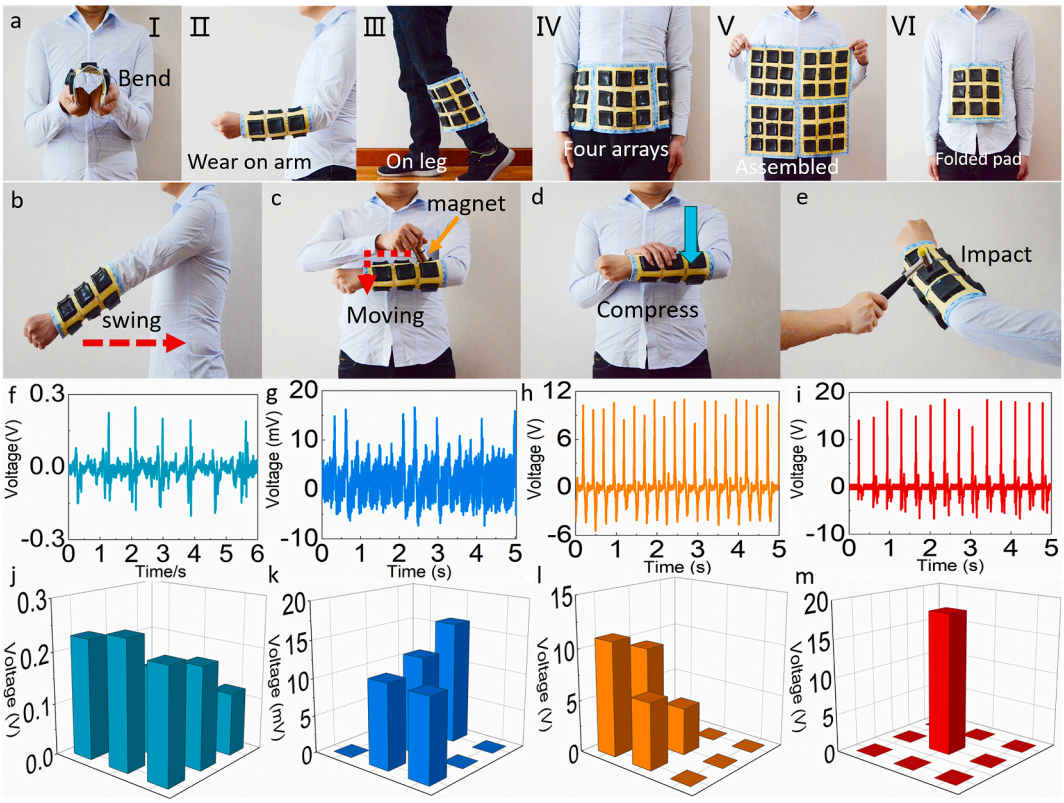

Fig. 7. (a) Shape programmable photographs of Kevlar/TENG device: (I) bendable, (II) worn on arm, (III) two arrays could be assembled and worn on leg, (IV) four assembled arrays were wrapped on waist, (V) the arrays were integrated into one pad with larger protection area and (VI) the overlying one provided higher protection effect. (b) Self-powered sensing properties of the array under arm swing, (c) magnetic attraction, (d) compression, (e) impact, (j–m) the corresponding voltage variation distribution and (f–i) the stable maximum voltage-time curves, respectively.

advanced TENG towards smart glove and wearable e-textile with multi-mode energy harvesting, safeguarding and self-powered external-field monitoring properties enabled to precisely mapping different external stimuli. This paper proposed a new avenue for the improvement of smart TENG as portable electronics in energy source, personal security and functional self-powered sensors.

CRediT authorship contribution statement

Sheng Wang: Investigation, Writing - original draft, Methodology, Visualization. **Shuai Liu:** Investigation, Formal analysis. **Jianyu Zhou:** Investigation, Data curation. **Faxin Li:** Formal analysis, Writing - review & editing. **Jun Li:** Visualization, Methodology. **Xufeng Cao:** Formal analysis, Computational simulation. **Zhiyuan Li:** Methodology. **Junshuo Zhang:** Investigation. **Binshang Li:** Formal analysis. **Yu Wang:** Software, Data curation. **Xinglong Gong:** Resources, Supervision, Project administration, Funding acquisition.

Declaration of competing interest

The authors declare that we have no competing financial interests or personal relationships that could have appeared to influence the work reported in this paper.

Acknowledgement

Financial supports from the National Natural Science Foundation of China (Grant No. 11802303, 11772320, 11972032, 11972337), the Strategic Priority Research Program of the Chinese Academy of Sciences (Grant No. XDB22040502), and China Postdoctoral Science Foundation (Grant No. 2018M632543, 2019T120544) are gratefully acknowledged.

Appendix A. Supplementary data

Supplementary data to this article can be found online at https://doi.org/10.1016/j.nanoen.2020.105291.

References

[1] H.J. Ryu, H.J. Yoon, S.W. Kim, Adv. Mater. 31 (2019) 1802898–1802917.
[2] J.H. Kim, Y. Lee, S. Cho, J. Gwon, H. Cho, M. Jang, S. Lee, S.Y. Lee, Energy Environ. Sci. 12 (2019) 177–186.
[3] X. Liu, K. Zhao, Z.L. Wang, Ya Yang, Adv. Energy Mater. 7 (22) (2017) 1701629–1701637.
[4] X.L. Wei, Z. Wen, Y.N. Liu, N.N. Zhai, A.M. Wei, K. Feng, G.T. Yuan, J. Zhong, Y. H. Qiang, X.H. Sun, Nano-Micro Lett. 12 (2020) 88–98.
[5] F. Fan, Z. Tian, Z. Wang, Nano Energy 1 (2012) 328–334.
[6] J. Huang, X. Yang, J. Yu, J. Han, C. Jia, M. Ding, J. Sun, X. Cao, Q. Sun, Z. Wang, Nano Energy 69 (2020) 104419–104427.
[7] X. Cao, Y. Jie, N. Wang, Z.L. Wang, Adv. Energy Mater. 6 (2016) 1600665–1600686.
[8] X.N. Wen, Y.J. Su, Y. Yang, H.L. Zhang, Z.L. Wang, Nano Energy 4 (2014) 150–156.
[9] H.Y. Guo, X.J. Pu, J. Chen, Y. Meng, M.H. Yeh, G.L. Liu, Q. Tang, B.D. Chen, D. Liu, S. Qi, C.S. Wu, C.G. Hu, J. Wang, Z.L. Wang, Sci. Robot. 3 (2018) 2516–2526.
[10] X. Cao, M. Zhang, J. Huang, T. Jiang, J. Zou, N. Wang, Z. Wang, Adv. Mater. 30 (2018) 1704077–1704085.
[11] Y. Shin, J. Lee, Y. Park, S. Hwang, H.G. Chae, H. Ko, J. Mater. Chem. A 6 (2018) 22879–22888.
[12] Y. Yang, H.L. Zhang, Z.H. Lin, Y.S. Zhou, Q.S. Jing, Y.J. Su, J. Yang, J. Chen, C. G. Hu, Z.L. Wang, ACS Nano 7 (10) (2013) 9213–9222.
[13] P. Cheng, M.C. Sun, C.L. Zhang, H.Y. Guo, J.H. Shi, Y. Zhang, Y. Liu, J. Wang, Z. Wen, X.H. Sun, IEEE Trans. Nanotechnol. 19 (2020) 230–235.
[14] K.Q. Xia, Z.Y. Zhu, H.Z. Zhang, C.L. Du, Z.W. Xu, R.J. Wang, Nano Energy 50 (2018) 571–580.
[15] Y. Jie, H. Zhu, X. Cao, Y. Zhang, N. Wang, L. Zhang, Z.L. Wang, ACS Nano 10 (2016) 10366–10372.
[16] Y.J. Su, Y. Yang, X.D. Zhong, H.L. Zhang, Z.M. Wu, Y.D. Jiang, Z.L. Wang, ACS Appl. Mater. Interfaces 6 (1) (2014) 553–559.
[17] K.Q. Xia, Z.Y. Zhu, H.Z. Zhang, C.L. Du, J.M. Fu, Z.W. Xu, Nano Energy 56 (2019) 400–410.

[18] W. Xu, H. Zheng, Y. Liu, X. Zhou, C. Zhang, Y. Song, X. Deng, M. Leung, Z. Yang, R. X. Xu, Z. Wang, X. Zeng, Z. Wang, Nature 578 (2020) 392–396.
[19] K. Zhao, Z.L. Wang, Y. Yang, ACS Nano 10 (9) (2016) 9044–9052.
[20] Y. Zhang, M.F. Peng, Y.N. Liu, T.T. Zhang, Q.Q. Zhu, H. Lei, S.N. Liu, Y. Tao, L. Li, Z. Wen, X.H. Sun, ACS Appl. Mater. Interfaces 12 (2020) 19384–19392.
[21] Y. Jie, Q. Jiang, Y. Zhang, N. Wang, X. Cao, Nano Energy 27 (2016) 554–560.
[22] Y.W. Feng, K. Han, T. Jiang, Z.F. Bian, X. Liang, X. Cao, H.X. Li, Z.L. Wang, Nano Res. 12 (2019) 2729–2735.
[23] G.L. Liu, H.Y. Guo, S.X. Xu, C.G. Hu, Z.L. Wang, Adv. Energy Mater. 9 (2019) 1900801–1900809.
[24] X. Liang, T. Jiang, G. Liu, T. Xiao, L. Xu, W. Li, F. Xi, C. Zhang, Z. Wang, Adv. Funct. Mater. 29 (2019) 1807421–1807429.
[25] X. Fan, J. He, J. Mu, J. Qian, N. Zhang, C. Yang, X. Hou, W. Geng, X. Wang, X. Chou, Nano Energy 68 (2020) 104319–104328.
[26] X. Wang, Z.L. Wang, Y. Yang, Nano Energy 26 (2016) 164–171.
[27] X. Liang, T. Jiang, G. Liu, Y. Feng, C. Zhang, Z. Wang, Energy Environ. Sci. 13 (2020) 277–285.
[28] Y. Liu, Y. Zheng, T. Li, D. Wang, F. Zhou, Nano Energy 61 (2019) 454–461.
[29] H. Wang, Z.L. Xiang, P. Giorgia, X.J. Mu, Y. Yang, Z.L. Wang, Nano Energy 23 (2016) 80–88.
[30] Q. Shi, H. Wang, H. Wu, C. Lee, Nano Energy 40 (2017) 203–213.
[31] K.Q. Xia, J.M. Fu, Z.W. Xu, Adv. Energy Mater. (2020) 2000426–2000435.
[32] X. He, Q. Wen, Y. Sun, Z. Wen, Nano Energy 40 (2017) 300–307.
[33] S. Qi, H. Guo, J. Chen, J. Fu, C. Hu, M. Yu, Z. Wang, Nanoscale 10 (2018) 4745–4752.
[34] Z. Wu, W. Ding, Y. Dai, K. Dong, C. Wu, L. Zhang, Z. Lin, J. Cheng, Z. Wang, ACS Nano 12 (2018) 5726–5733.
[35] X. Wang, Y. Yang, Nano Energy 32 (2017) 36–41.
[36] T. Quan, Y.C. Wu, Y. Yang, Nano Res. 8 (2015) 3272–3280.
[37] A. Ahmed, I. Hassan, I.M. Mosa, E. Elsanadidy, M. Sharafeldin, J.F. Rusling, S. Ren, Adv. Mater. 31 (2019) 1807201–1807211.
[38] Y. Zou, P. Tan, B. Shi, H. Ouyang, D. Jiang, Z. Liu, H. Li, M. Yu, C. Wang, X. Qu, L. Zhao, Y. Fan, Z. Wang, Z. Li, Nat. Commun. 10 (2019) 2695–2705.
[39] A. Mongera, P. Rowghanian, H.J. Gustafson, E. Shelton, D.A. Kealhofer, E.K. Carn, F. Serwane, A.A. Lucio, J. Giammona, O. Campas, Nature 561 (2018) 401–406.
[40] I. Peters, S. Majumdar, H.M. Jaeger, Nature 532 (2016) 214–217.
[41] N. Park, V. Rathee, D. Blair, J. Conrad, Phys. Rev. Lett. 122 (2019) 228003–228009.
[42] H. Zhang, X. Zhang, Q. Chen, X. Li, P. Wang, E. Yang, F. Duan, X. Gong, Z. Zhang, J. Yang, J. Mater. Chem. A 5 (2017) 22472–22479.
[43] M. Liu, S. Zhang, S. Liu, S. Cao, S. Wang, L. Bai, M. Sang, S. Xuan, W. Jiang, X. Gong, Compos. Part A. 126 (2019) 105612–105618.
[44] Q. He, Y. Wu, Z. Feng, W. Fan, Z. Lin, C. Sun, Z. Zhou, K. Meng, W. Wu, J. Yang, J. Mater. Chem. A 7 (2019) 26804–26811.
[45] W.L. Liu, Z. Wang, G. Wang, Q.X. Zeng, W.C. He, L.Y. Liu, X. Wang, Y. Xi, H.Y. Guo, C.G. Hu, Z.L. Wang, Nat. Commun. 11 (2020) 1883–1893.
[46] Y. Yang, H.L. Zhang, Z.L. Wang, Adv. Funct. Mater. 24 (2014) 3745–3750.
[47] H.X. Jiang, H. Lei, Z. Wen, J.H. Shi, D.Q. Bao, C. Chen, J.X. Jiang, Q.B. Guan, X. H. Sun, S.T. Lee, Nano Energy 75 (2020) 105011–105018.
[48] J. Nie, Z. Ren, L. Xu, S. Lin, F. Zhan, X. Chen, Z. Wang, Adv. Mater. 32 (2020) 1905696–1905707.
[49] T. Hu, S. Xuan, L. Ding, X. Gong, Mater. Des. 156 (2018) 528–537.
[50] S. Wang, S. Xuan, Y. Wang, C. Xu, Y. Mao, M. Liu, L. Bai, W. Jiang, X. Gong, ACS Appl. Mater. Interfaces 8 (2016) 4946–4954.
[51] S. Sundaram, P. Kellnhofer, Y. Li, J. Zhu, A. Torralba, W. Matusik, Nature 569 (2019) 698–702.
[52] S. Wang, L. Gong, Z. Shang, L. Ding, G. Yin, W. Jiang, X. Gong, S. Xuan, Adv. Funct. Mater. 28 (2018) 1707538–1707547.
[53] A. Hazarika, B.K. Deka, C. Jeong, Y.B. Park, H.W. Park, Adv. Funct. Mater. 29 (2019) 1903144–1903156.

Sheng Wang received his Ph. D. degree from University of Science and Technology of China in 2017. Now he is a postdoctoral fellow in the Chinese Academy of Sciences Key Laboratory of Mechanical Behavior and Design of Materials in Hefei, China. His research interests include smart materials and devices with magnetic, electric and force-sensing properties. He is also interested in developing multifunctional triboelectric nanogenerator systems.

Shuai Liu received his Bachelor degree in the Department of Modern Mechanics from University of Science and Technology of China, Hefei, Anhui, P.R. China in 2019. He is currently a Master candidate under the supervision of Prof. Xinglong Gong and Prof. Shouhu Xuan in the Intelligent Materials and Vibration Control Laboratory at the same school. His research interests focus on the development and application of multifunctional magnetic materials and their devices.

Jianyu Zhou received his B.S. degree in Engineering Mechanics (Qian Lingxi Excellence in Education Program) from Dalian University of Technology in 2019. He is currently a postgraduate in Department of Modern Mechanics at University of Science and Technology of China. His research interests are focused on anti-impact devices and smart textile materials.

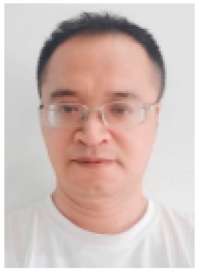

Faxin Li obtained his Ph.D degree on solid mechanics from Tsinghua University in 2004. He finished his postdoctoral training in 2007 at the University of British Columbia, Canada, with Prof. Nimal Rajapakse. In Oct. 2007, he joined College of Engineering, Peking University and became a full professor in 2014. His research focus is on the mechanics of smart materials and structures, guided wave based structural health monitoring. He served as an Associate Editor of the IOP journal "Smart Materials and Structures" since 2015.

Jun Li received his Master degree of Senior Business Administration from Peking University. Now he is the general manager in Weiwei Group Co., Ltd. As a technical expert, he winned many awards such as Technology Leader in Anhui Province, Science and Technology Innovation Award. His research interests include the synthesis of polymer composites and application of smart materials, such as vibration control and machine dynamics.

Xufeng Cao received his Bachelor degree in Engineering Mechanics from Northwestern Polytechnical University, Xi'an, P. R. China in 2017. He is currently a Ph.D. candidate in Department of Modern Mechanics at University of Science and Technology of China. His research interests are focused on the structural design, simulation and application of intelligent magnetic materials.

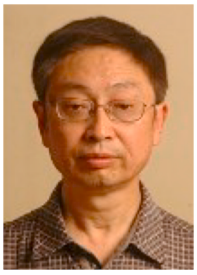

Zhiyuan Li graduated from Hefei University of Technology in 1982 and then worked as a teacher. During 1991 to 1994, he studied in University of Stuttgart in Germany. Now as a doctor supervisor and director of the Noise Vibration Laboratory in Hefei University of Technology, his research interests include the function design of polymer and the application of intelligent materials in vibration control and machine dynamics. He is also the Chairman of Institute of Vibration Absorption in Weiwei Glue Parts Group Co., Ltd.

Junshuo Zhang received his bachelor degree from University of Science and Technology of China and continued his research under the direction of Prof. Xinglong Gong in the Intelligent Materials and Vibration Control Laboratory. His research focuses on novel shear thickening fluid and the mechanical properties of smart textiles.

Bingshang Li is the Chairman of Anhui Weiwei Glue Parts Group Co., Ltd in China and the President of Chamber of Fangang Commerce. He is the technology leader in Anhui Province. He was also honored as Innovative Entrepreneur in Tongcheng City, Science and Technology Award. His research interests include the design of intelligent polymer and their applications in vibration control and machine dynamics.

Yu Wang is an Associate Professor in the Department of Modern Mechanics, University of Science and Technology of China (USTC). He received his B.Sc. and Ph.D. from the USTC. After graduation, he also worked as a visiting scholar in Hong Kong University of Science and Technology for 1 year. Dr. Wang's research interests include on the mechanical behaviors and its constitutive characterization of soft materials with the multi-physics coupling properties for sensing and safeguard application.

Dr. **Xinglong Gong** received his Ph.D. degree in Mechanics from both the University of Science and Technology of China (USTC, China) and Saitama University (Japan), in 1996. Then, he worked at the Nihon Dempa Kogyo Co., Ltd., Japan. In 2003, he joined the Department of Modern Mechanics, USTC, as a Full Professor. He is currently the council chairman of Chinese Society of Experimental Mechanics. His research interests comprise soft matter materials as well as their applications. He was supported by the 100-Talent Programme of Chinese Academy of Sciences in 2003 and supported by the National Science Foundation for Distinguished Young Scholars of China in 2011.